



## CENTRE DE RECERCA MATEMÀTICA

This is a preprint of: *Stochastic modelling of viral blips in HIV-1-infected patients: Effects of inhomogeneous density fluctuations*

Journal Information: *Journal of Theoretical Biology*,

Author(s): D. Sanchez-Taltavull and T. Alarcon.

Volume, pages: 371 1-11, DOI:[[doi.org/10.1016/j.jtbi.2015.02.001](https://doi.org/10.1016/j.jtbi.2015.02.001)]



# Stochastic modelling of viral blips in HIV-1-infected patients: Effects of inhomogeneous density fluctuations



Daniel Sánchez-Taltavull <sup>a,b,\*</sup>, Tomás Alarcón <sup>a,c</sup>

<sup>a</sup> Centre de Recerca Matemàtica, Edifici C, Campus de Bellaterra, 08193 Bellaterra (Barcelona), Spain

<sup>b</sup> Departament de Matemàtica Aplicada i Anàlisi, Universitat de Barcelona, 08007 Barcelona, Spain

<sup>c</sup> Departament de Matemàtiques, Universitat Autònoma de Barcelona, 08193 Bellaterra (Barcelona), Spain

## AUTHOR - HIGHLIGHTS

- We present a stochastic inhomogeneous model of HIV-1 dynamics.
- Viral blips are product of random fluctuations.
- Viral blips are strongly influenced by laboratory artifacts.

## ARTICLE INFO

### Article history:

Received 28 July 2014

Received in revised form

28 January 2015

Accepted 1 February 2015

Available online 11 February 2015

### Keywords:

Latent infection

HAART

Viral persistence

Viral replication

Laboratory procedures

## ABSTRACT

We propose a stochastic model of HIV-1 infection dynamics under HAART in order to analyse the origin and dynamics of the so-called viral blips, i.e. episodes of transient viremia that occur in the phase of where the disease remains in a latent state during which the viral load raises above the detection limit of standard clinical assays. Based on prior work in the subject, we consider an infection model in which latently infected cell compartment sustains a residual (latent) infection over long periods of time. Unlike previous models, we include the effects of inhomogeneities in cell and virus concentration in the blood stream. We further consider the effect of burst virion production. By comparing with the experimental results obtained during a study in which intensive sampling was carried out on HIV-1-infected patients undergoing HAART over a long period of time, we conclude that our model supports the hypothesis that viral blips are consistent with random fluctuations around the average viral load. We further observe that agreement between our simulation results and the blip statistics obtained in the aforementioned study improves when burst virion production is considered. We also study the effect of sample manipulation artifacts on the results produced by our model, in particular, that of the post-extraction handling time, i.e. the time elapsed between sample extraction and actual test. Our results support the notion that the statistics of viral blips can be critically affected by such artifacts.

© 2015 Elsevier Ltd. All rights reserved.

## 1. Introduction

HIV infection is effectively controlled by administration of anti-retroviral therapy (ART). Despite the great success of highly-active ART (HAART), the goal of curing, in the sense of completely eradicating, HIV-1 infection is yet to be achieved (Richman et al., 2009). Quantitative analysis of the temporal evolution of plasma viral load upon HAART treatment suggests the existence of several phases in the therapy-induced decay of the viral load (Pierson et al., 2000; Kim and Perelson, 2006; Rong and Perelson, 2009b).

After an initial shoulder, reflecting delays associated to both the pharmacokinetics and the production of virus by newly infected cells (Perelson et al., 1996; Herz et al., 1996), a first phase of fast exponential decline of the viral load is observed where viral load is reduced by one to two orders of magnitude over a period of time of approximately two weeks. This fast response stage, with half-life time of the order of days, reflects short half-life time of plasma virus and of productively infected CD4<sup>+</sup> T lymphocytes (Ho et al., 1995; Wei et al., 1995; Markowitz et al., 2003). Following this initial phase of fast decline in plasma viral load, a second stage of slower decay starts with a half-life time between one and four weeks. This phase reflects the contribution to virus load of infected cells with longer half-life time, such as macrophages, and infected CD4<sup>+</sup> T cells that exhibit a lower rate of viral replication (Perelson

\* Corresponding author. Tel.: +34 93 581 3102.

E-mail address: [dsanchez@crm.cat](mailto:dsanchez@crm.cat) (D. Sánchez-Taltavull).

et al., 1997; Ho et al., 1986; Zhang et al., 1999). After this second stage, plasma virus load has normally fallen below the detection threshold of standard clinical assays ( $\sim 50$  RNA copies/ml). However, following this second phase, HAART appears to fail to completely eradicate the infection. Rather, a third stage ensues with much longer half-life time than the previous ones (of the order of months or even years (Kim and Perelson, 2006) in which residual levels of viral load (as low as 1–5 copies RNA/ml detectable only by supersensitive assays) persist in plasma as well as in other bodily compartments, such as semen.

The question of what is the source of this residual viral load has triggered much debate which has materialised in several working hypothesis. One of these hypothesis invokes the possibility that HAART is not completely suppressive thus allowing the infection to continue to replicate in anatomical HIV-1 reservoirs (Pierson et al., 2000), in particular within the so-called “drug sanctuaries”, i.e. sites of poor drug penetration where the infection is allowed to persist (Kepler and Perelson, 1998).

An alternative model suggests that, a cellular reservoir exists which allows the infection to linger in latent form with residual viral load being the result of the activation of the latently infected cells (Pierson et al., 2000). Such a latent reservoir is established within the population of infected CD4+ T memory cells (Chun et al., 1995, 1997) and, therefore, they remain in the resting state in the presence of HAART for prolonged periods of time. As a consequence, latently infected cells are able to escape the effect of the drug and immune surveillance due to the fact that they undergo no duplication and, consequently, exhibit very low levels of HIV-1 messenger RNA (Rong and Perelson, 2009b). However, since latently infected cells release virus when stimulated with the proper antigen, viral rebound will eventually occur when HAART is withdrawn leading to HIV-1 infection recurrence, consistent with a wider scenario of quiescence-induced escape (Alarcon and Jensen, 2010).

Once HAART has forced the infection to enter the latent stage, one can observe transient episodes of viremia where the viral load raises above the standard test detection limit (50 copies mRNA/ml) for a brief period of time (Dornadula et al., 1999; Ramratnam et al., 1999; Havlir et al., 2001; Nettles et al., 2005). These episodes are referred to as *blips*. The origin and clinical relevance of these blips remains unclear and a number hypothesis have been formulated (Rong and Perelson, 2009b). An early hypothesis regarding the origins of such blips, whose emergence was, at the time, suspected of heralding imminent virological failure, was that they are due to the appearance of new, drug-resistant viral variants (Macias et al., 2005). However, a number of studies have compiled evidence against viral blips being correlated with virological failure (Havlir et al., 2001; Mira et al., 2002; Nettles et al., 2005), thus weakening the case of viral blips being early warnings related to viral evolution leading to drug resistant strains of the virus. Further to the hypothesis of blips being originated by viral evolution, other mechanisms have been proposed which include antigen-driven CD4+ T cell activation due to vaccination or secondary infections (Ferguson et al., 1999; Gunthard et al., 2000; Frazer et al., 2001; Fraser et al., 2001; Frenkel et al., 2003; Jones and Perelson, 2002, 2005). It has also been shown that activation of latently infected cells may play a role in the emergence of viral blips. For example, Jones & Perelson have proposed a model in which increased activation of latently infected cells can lead to a burst in viral load (Jones and Perelson, 2007). The possibility that asymmetric division of activated latently infected cells may help to explain the decay kinetics of the latent compartment and intermittent viral blips has been explored in Rong and Perelson (2009c). Recently, Rong and Perelson (2009b) have formulated a model in which stochastic activation of latently infected cells can maintain viral blips without completely depleting the latent reservoir, thus

maintaining long-term, low-level viremia. They also developed a model which incorporated density-dependent homeostatic proliferation of the memory CD4+ T memory cells (and, therefore, of the latently infected cell compartment), which, according to Chomont et al. (2009), drives persistence and determines the size of the latent reservoir. Recently, a model which includes a stochastic population switch of the latently infected cells has been developed to study the persistence of the latent reservoir and the viral blips (Wang and Rong, 2014).

Alongside all these models which postulate that viral blips have a physiological origin, there is an alternative school of thought which claims that most viral blips are random occurrences of probabilistic origin related to the small number of virus copies in the latent phase as well as being partly produced by laboratory artefacts during the processing of the samples (Lee et al., 2006; Nettles and Kieffer, 2006). According to this view, viral blips are mostly uncorrelated with virological failure, virus evolution, vaccination, or non-adherence to treatment regimen (Nettles et al., 2005; Lee et al., 2006; Nettles and Kieffer, 2006) and, therefore, only a small fraction of such occurrences are of clinical significance. Conway and Coombs (2011) have proposed a model to analyse the stochastic viral dynamics in treated patients. This model treats viral blips as random events occurring every time the viral load reaches the standard detection limit (i.e. 50 mRNA/ml). Although this model reproduces many of the features of HIV-1 viral dynamics and provides a detailed description of its stochastic dynamics, there are several properties of the statistics of viral blips in which Conway and Coombs (2011) appears to depart from experimental observation. One such departure refers to the frequency of blips. According to the model formulated in Conway and Coombs (2011), blip frequency decreases exponentially in time which disagrees with the results by DiMascio et al. (2003) where a constant blip rate is reported. Conway and Coombs (2011) claim that this difference is due to the fact that, whilst their model accounts only for blips of small amplitude caused by fluctuations, DiMascio et al. (2003) include in their statistics blips of both small and large amplitude. Therefore, Conway & Coombs implicitly assume that large blips must have a biological origin. Furthermore, the data collected by Nettles et al. (2005), where intensive sampling was carried out on HIV-1-infected patients with samples collected every 2–3 days over a period of 3–4 months, reported that blips were observed in 9 out of 10 patients with an average of two blips per patient. The blip statistics produced by the model formulated in Conway and Coombs (2011) appears to predict blips be too rare to be comparable to the experimental data, even in conditions of elevated virus rate production and latent cell activation. It can be argued that the rationale for this discrepancy is the same as before: Nettles et al. (2005) measure the full range of blips (both small and large amplitudes) whilst Conway and Coombs (2011) account only for small-amplitude blips. Therefore, according to this model (Conway and Coombs, 2011), small amplitude blips are consistent with a stochastic model whereas large amplitude blips must be produced by causes other than random fluctuations.

One common feature shared by all of the models discussed so far, both stochastic and deterministic, is that they all assume that the system is well-mixed, i.e. all the cellular and molecular species are evenly distributed over the volume of blood so that only the number of each species determines the state of the system. For this modelling assumption to hold, the numbers of each species must be large enough so that their densities remain approximately uniform. The system we are dealing with in this paper has at least two species, virus and infected cells, which are present in very small numbers. As a consequence, their densities can show large fluctuations which would lead to large inhomogeneities in the local numbers of such species. The effect of this inhomogeneity can be rather sizeable, specially since measurements of viral load

are performed by extracting small samples of blood which are then analysed.

The aim of this paper is to ascertain whether density fluctuations affect the stochastic dynamics of the viral load in HAART-treated patients beyond the predictions of reference (Conway and Coombs, 2011) and investigate if a stochastic model which includes density fluctuations is capable of a more faithful reproduction of the experimental results reported in DiMascio et al. (2003); Nettles et al. (2005). To this end we formulate a stochastic compartmental model (Bernstein, 2005) where volume of blood is divided in small compartments (whose volume is assumed of the order of the volume of one blood sample taken for analysis). Within each of these compartments, the system is assumed to be well-mixed but we consider that differences may arise between compartments thus accounting for density fluctuations (Gibson and Bruck, 2000; Elf and Ehrenberg, 2004; Elgart and Kamenev, 2004; Erban et al.; Lugo and McKane, 2008; Spill et al., 2015). Furthermore, in order to address the issue of whether laboratory artefacts alter the statistics of viral blips we have designed an *in silico* blood extraction procedure that allows us to study, at least partially, this aspect of the problem.

This paper is organised as follows. Section 2 is devoted to a detailed explanation of the model assumptions and formulation. In Section 3 we conduct extensive simulations of our model and present our results. Finally, Section 4 we proceed to discuss our results and compare, to the extent that this is possible, with experimental results.

## 2. Model formulation

We now proceed to present our compartmental model of stochastic viral dynamics. Our model is based on the modelling approach whereby spatially inhomogeneous systems are dealt with by compartmentalising the domain where the system lives into small compartments (Bernstein, 2005). Within each of these compartments all of the species participating in the dynamics of the system are assumed to be well-mixed, so that our resolution to measure spatial variations is of the order of the compartment size. The local, well-mixed, within-compartment stochastic dynamics is supplemented by stochastic transitions that allow for transport of species between compartments. This approach has been widely applied to many situations in which spatial heterogeneity is essential, in particular, reaction-diffusion systems (Gibson and Bruck, 2000; Elf and Ehrenberg, 2004; Elgart and Kamenev, 2004; Erban et al.; Lugo and McKane, 2008; Spill et al., 2015). This setting will allow us to ascertain the effect of density fluctuations on stochastic viral dynamics.

Further to our compartmental model, we also formulate an *in silico* blood analysis model, which intends to follow as closely as possible the intensive sampling procedure designed by Nettles et al. (2005) to analyse the dynamics and statistics of viral blips in HIV-1-infected patients under HAART.

### 2.1. Compartmental model

In order to account for density fluctuations, we consider a compartmental model, schematically shown in Fig. 1. We will assume that, in an attempt to roughly imitate the structure of the blood stream, compartments are arranged on a one dimensional, closed (i.e. with periodic boundary conditions) lattice (see Fig. 1). In each compartment, we consider three types of interacting species, namely, active infected cells, latently infected cells, and virus. The number of each of these species in compartment  $i$  is referred to as  $T_i^*$ ,  $L_i$ , and  $V_i$ , respectively, where  $i = 1, \dots, N_c$  with  $N_c$  is the number of compartments. We further introduce the vector

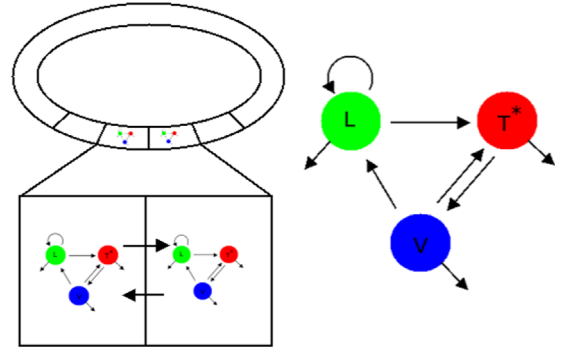


**Fig. 1.** This figure depicts a schematic diagram of our compartmental model. Our model represents the circulatory system in a very simplistic way as a one dimensional closed circuit of adjacent compartments. Within each compartment we model the (local) cellular dynamics of an HIV-1-infected T-cell population with latency (Rong and Perelson, 2009a; Conway and Coombs, 2011): we consider the dynamics of the HIV-1 virus load ( $V$ ), productively infected T-cells ( $T^*$ ), and latently infected cells ( $L$ ). Virus capsids,  $V$ , are released by productively infected cells and has the virus that can infect the uninfected T-cells. We consider that the number of uninfected T-cells is so much larger than that of infected cells that we consider them as a reservoir. Latently infected cells can become active upon stimulation with proper antigens. In addition to this within-compartment cellular dynamics, we consider random movement of both latently and active infected cells and virus capsids between compartments.

$X(t) \equiv (T_1^*(t), L_1(t), V_1(t), \dots, T_{N_c}^*(t), L_{N_c}(t), V_{N_c}(t))$  whose components correspond to the number of cells of each species at site  $i = 1, \dots, N_c$  and time  $t$ . We will find convenient to define  $x_i(t) \equiv (T_i^*(t), L_i(t), V_i(t))$ , so that the vector  $X(t)$  can be written as  $X(t) = (x_1(t), \dots, x_{N_c}(t))$ .

The stochastic dynamics of our system is described by the corresponding Master Equation (Van Kampen, 2007; Lugo and McKane, 2008; Gardiner, 2009):

$$\frac{\partial}{\partial t} P(X, t) = \sum_{i=1}^{N_c} \sum_{j=1}^{R_L} (W_{j+(i-1)R_L}(X - r_{j+(i-1)R_L}) P(X - r_{j+(i-1)R_L}) - W_{j+(i-1)R_L}(X) P(X)) \\ + \sum_{i=1}^{N_c} \sum_{j=1}^{R_T} (\omega_{j+(i-1)R_T}(X - \rho_{j+(i-1)R_T}) P(X - \rho_{j+(i-1)R_T}) - \omega_{j+(i-1)R_T}(X) P(X)) \quad (1)$$

where we have splitted the Master Equation in a purely local part, corresponding to the population dynamics within each compartment, and a transport part, which accounts for transport of species between adjacent compartments.  $R_L$  and  $R_T$  are the number of local and transport events, respectively, that can affect the state,  $x_i$ , of each compartment. The transition rates are defined in Tables 1 and 2.

In order to facilitate later formulation of our *in silico* blood extraction protocol and its comparison with Nettles et al. (2005), we will consider compartments of volume  $V_c = 8.5$  ml each, which is the volume of blood sampled extracted for analysis in the study reported in Nettles et al. (2005). We will consider that an average individual has 5 litres of blood so we need to consider  $N_c = 588$  compartments.

The within-compartment stochastic viral dynamics model is based on previous works by Rong and Perelson (2009a) and Conway and Coombs (2011) and it is schematically shown in Fig. 1. Following the latter, we assume that, due to the large numbers in which CD4+ T uninfected cells are present, they are unaffected by fluctuations and their number is taken as constant. We assume that two types of infected cells exist, latently infected cells,  $L_i$ , which carry the virus but do not synthesize new virions, and active infected cells,  $T_i^*$ , which produce and release new virions. As a consequence, active infected cells are targeted by HAART whereas latently infected cells are immune to its effects. Both types of infected cells are produced by infection of uninfected T cells. Furthermore, latently infected cells can become active, for

example, by stimulation with appropriate antigens. Both latently and active infected cells are assumed to die at a certain rate and blood-borne virions are assumed to be cleared off at a constant rate. We also account for experimental results showing that the latently infected cells are maintained by homeostatic proliferation (Chomont et al., 2009), by means of a phenomenological model which includes branching and binary annihilation of latently infected cells (Rong and Perelson, 2009a; Elgart and Kamenev, 2004). There are evidences, reported in Siliciano et al. (2003), according to which the latent reservoir is decaying. Some extra reactions should be included in the compartmental model to reproduce this long-term decay. However, this has not been included in the model because the decay is very slow, and its effect in the short-time dynamics is negligible.

The elementary events involved in our spatial model of stochastic viral dynamics are as follows.

- Latently infected cells  $L_i$  can undergo
  1. Homeostatically balanced proliferation: Following Rong and Perelson (2009a), we account for homeostatic control of proliferation by means of a combination of branching ( $L_i \rightarrow 2L_i$ ) with binary annihilation ( $L_i + L_i \rightarrow \emptyset$ ). Although binary annihilation has no direct biological meaning in the present context, it has been shown (see e.g. Elgart and Kamenev, 2004) that, combined with branching, is a stochastic counterpart of the standard logistic growth, commonly used to model growth dynamics (Tsoularis and Wallace, 2002). The corresponding transition rates are  $W_{3+(i-1)R_L}$  for branching and  $W_{4+(i-1)R_L}$  for binary annihilation (see Table 1).
  2. Death: We assume a simple linear decay with transition rate  $W_{5+(i-1)R_L}$  as shown in Table 1.
  3. Activation: By means of this process a latently infected cell becomes an active infected cell  $L_i \rightarrow T_i^*$ . The corresponding transition rate is  $W_{6+(i-1)R_L}$ , Table 1.
  4. In addition to the processes described above, which have to do with the (within-compartment) population dynamics, we assume that latently infected cells can move between neighbouring compartments. We will assume a coupling between compartments where transitions occur at constant per cell rate,  $\nu_L$ . In periodic, one dimensional setting, cells in compartment  $i$  can move to compartment  $i+1$  at rate  $\omega_{1+(i-1)R_T}$  or to compartment  $i-1$  at rate  $\omega_{2+(i-1)R_T}$  as defined in Table 2.
- Active infected cells,  $T_i^*$ , cell are subjected to
  1. Apoptosis with transition rate  $W_{7+(i-1)R_L}$  (see Table 1).
  2. Virion production: Contrary to latently infected cells, active infected cells synthesise and release new virions. In general, viral production can occur in a continuous fashion over the life span of an infected cell or in a burst which kills the cell.

For the HIV infection both modes have been proposed (Pearson et al., 2011). Transition rate  $W_{9+(i-1)R_L}$  (Table 1) corresponds to continuous production. Later in the paper, we consider an additional scenario, in which both continuous and burst production occur.

3. Transport between neighbouring compartments. Just as latently infected cells do, active infected cells can move between compartments at rates  $\omega_{3+(i-1)R_T}$  and  $\omega_{4+(i-1)R_T}$  as per Table 2.

- Finally, virus,  $V_i$ , can

1. Infect a healthy T cell producing a latently infected cell. In patients under HAART, the infection process is hindered by the presence of an antiretroviral drug. The efficiency of such drug is measured by a parameter,  $\epsilon$ , which takes values between 0 and 1, the latter (former) corresponding to a maximally (in)efficient drug.  $(1-\epsilon)$  is interpreted as the proportion of virions capable of infection under HAART treatment. We also assume that, upon infection, the cell can become latently infected with probability  $\eta$  or active with probability  $(1-\eta)$ . Therefore the corresponding transition rate  $W_{1+(i-1)R_L}$  is proportional to  $\eta(1-\epsilon)$  as shown in Table 1.
2. Infect a healthy T cell producing an active infected cell. In this case, the corresponding transition rate  $W_{2+(i-1)R_L}$  is proportional to  $(1-\eta)(1-\epsilon)$  (see Table 1).
3. Undergo clearance. Virions are removed from the blood, which we model as a simple linear decay with transition rate  $W_{8+(i-1)R_L}$  as per Table 1.
4. Fail to infect and being eliminated by the drug with transition rate  $W_{10+(i-1)R_L}$  (see Table 1).
5. Transport between neighbouring compartments. Virions can move between compartments at rates  $\omega_{5+(i-1)R_T}$  and  $\omega_{6+(i-1)R_T}$  as per Table 2).

**Numerical methodology:** We will perform numerical simulations of the Master Equation (1) using the methodology proposed

**Table 2**

Transition rate corresponding to the stochastic model of viral blip generation. A detail is given in the main text (Section 2).  $R_T=6$ .

Transition rate	$\rho_{j+(i-1)R_T}$	Description
$\omega_{1+(i-1)R_T} = \mu_L + L_i$	$(0, \dots, 0, -1, 0, 0, 1, 0, \dots)$	$L_i + L_{i+1} \rightarrow L_i - 1 + L_{i+1} + 1$
$\omega_{2+(i-1)R_T} = \mu_L - L_i$	$(0, \dots, 0, 1, 0, 0, -1, 0, \dots)$	$L_i + L_{i-1} \rightarrow L_i - 1 + L_{i-1} + 1$
$\omega_{3+(i-1)R_T} = \mu_T^* + T_i^*$	$(0, \dots, 0, -1, 0, 0, 1, 0, \dots)$	$T_i^* + T_{i+1}^* \rightarrow T_i^* - 1 + T_{i+1}^* + 1$
$\omega_{4+(i-1)R_T} = \mu_T^* - T_i^*$	$(0, \dots, 0, 1, 0, 0, -1, 0, \dots)$	$T_i^* + T_{i-1}^* \rightarrow T_i^* - 1 + T_{i-1}^* + 1$
$\omega_{5+(i-1)R_T} = \mu_V + V_i$	$(0, \dots, 0, -1, 0, 0, 1, 0, \dots)$	$V_i + V_{i+1} \rightarrow V_i - 1 + V_{i+1} + 1$
$\omega_{6+(i-1)R_T} = \mu_V - V_i$	$(0, \dots, 0, 1, 0, 0, -1, 0, \dots)$	$V_i + V_{i-1} \rightarrow V_i - 1 + V_{i-1} + 1$

**Table 1**

Transition rates corresponding to the stochastic model of viral blip generation. See text (Section 2) for details.  $R_L=10$ .  $T_i$ , the number of uninfected cells is taken to be constant (Conway and Coombs, 2011).  $\Omega$  is the compartment size.

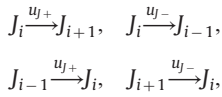
Transition rate	$r_{j+(i-1)R_L} = (\Delta L_i, \Delta T_i^*, \Delta V_i)$	Description
$W_{1+(i-1)R_L} = \eta(1-\epsilon)kV_iT_i\Omega^{-1}$	$(1, 0, -1)$	Latent infection $T_i + V_i \rightarrow L_i$ cell
$W_{2+(i-1)R_L} = (1-\eta)(1-\epsilon)kV_iT_i\Omega^{-1}$	$(0, 1, -1)$	Active infection $T_i + V_i \rightarrow T_i^*$ cell
$W_{3+(i-1)R_L} = rL_i$	$(1, 0, 0)$	Latent cell proliferation $L_i \rightarrow 2L_i$
$W_{4+(i-1)R_L} = \frac{r}{L_{max}} \frac{L_i(L_i-1)}{2} \Omega^{-1}$	$(-2, 0, 0)$	Latent cell binary annihilation $L_i + L_i \rightarrow \emptyset$
$W_{5+(i-1)R_L} = d_0L_i$	$(-1, 0, 0)$	Latent cell clearance $L_i$
$W_{6+(i-1)R_L} = a_iL_i$	$(-1, 1, 0)$	Activation $L_i \rightarrow T_i^*$
$W_{7+(i-1)R_L} = \delta T_i^*$	$(0, -1, 0)$	Active cell death
$W_{8+(i-1)R_L} = cV_i$	$(0, 0, -1)$	Virion clearance
$W_{9+(i-1)R_L} = p_V T_i^*$	$(0, 0, 1)$	Continuous virion production
$W_{10+(i-1)R_L} = \epsilon kV_iT_i\Omega^{-1}$	$(0, 0, -1)$	Failed infection



by Bernstein (2005), which is a straight forward generalisation of the original stochastic simulation algorithm proposed by Gillespie (1976). We have chosen the methodology which, by generating exact sample paths of our stochastic dynamics, allows us the most direct comparison with the experimental procedure of Nettles et al. so that we could focus on possible mechanisms and causes of viral blips. We estimated that direct compartmental-SSA simulations as the most effective means to accomplish this comparison, rather than using, for example, the methodology Conway and Coombs (2011) put forward.

We examine an application of the Gillespie algorithm to simulating spatially inhomogeneous reaction–diffusion systems in mesoscopic volumes such as cells and microchambers. The method involves discretizing the chamber into elements and modeling the diffusion of chemical species by the movement of molecules between neighbouring elements. These transitions are expressed in the form of a set of reactions which are added to the chemical system.

Our numerical method is an application of the generalisation of the Gillespie algorithm proposed in Bernstein (2005) to simulating spatially inhomogeneous reaction–diffusion systems in mesoscopic. The method involves discretising the simulation volume into elements of volume  $\Omega$  and modelling the diffusion of chemical species by the movement of molecules between neighbouring elements. These transitions are expressed in the form of a set of reactions which are added to the chemical system. Thus, within the  $i$ -th compartment, we consider the populations  $L_i, T_i^*, V_i$  to evolve as determined by the local reaction channels given by Table 1, where the volume  $\Omega = V_c$ , is the volume of the compartment. In addition to these reactions, we consider the transport reactions of the form:



where  $J = V, L, T^*$ , and the transition rates  $u_{j\pm}$  are chosen as shown in Table 2, so that the mean-field limit corresponds a discretised reaction–diffusion system with biased diffusion (see Section 2.2 below).

**Parameter values:** The (default) parameter values used in our simulations are given in Table 3. The parameter values corresponding to the model of cellular dynamics of an HIV-1-infected T-cell population with latency are based on estimates available in the literature on the subject.

Random motility between compartments has been modelled as simple diffusion. The transition probability between compartments is therefore given by  $\mu_{j\pm} = D_j/h^2$ , where  $J = V, L, T^*$ ,  $D_j$  is the diffusion coefficient of species  $J$ , and  $h = \sqrt[3]{V_c}$ , where  $V_c$  is the

compartment volume. The magnitude of the diffusion coefficient for several types of viral capsids has been estimated between 1.6 and  $30 \mu\text{m}^2 \text{s}^{-1}$  (Murray and Jackson, 1992). We consider a typical value  $D_v = 5 \mu\text{m}^2 \text{s}^{-1}$  (Hille, 1992; Berg, 1993). Similarly, we take a generic estimate for the diffusion coefficient of a cell  $D_L = D_{T^*} = 0.05 \mu\text{m}^2 \text{s}^{-1}$  (Bray, 2001). Furthermore, in order to account for the directionality of blood flow, we assume that  $\mu_{j-} = 3\mu_{j+}$ .

## 2.2. Mean-field dynamics

As a first approach to the dynamics, we study the mean-field behaviour of this system, which is given by the following differential equations:

$$\begin{aligned} \frac{dL_i}{dt} &= \eta(1-\epsilon)kV_iT + rL_i \left(1 - \frac{L_i}{L_{\max}}\right) - a_L L_i - d_L L_i \\ &\quad - (\mu_{L+} + \mu_{L-})L_i + \mu_{L+}L_{i-1} + \mu_{L-}L_{i+1}, \\ \frac{dT_i^*}{dt} &= (1-\eta)(1-\epsilon)kV_iT + a_L L_i - \delta T_i^* - (\mu_{T+} + \mu_{T-})T_i \\ &\quad + \mu_{T+}T_{i-1} + \mu_{T-}T_{i+1}, \\ \frac{dV_i}{dt} &= p_v T_i^* - cV_i - ckTV_i - (\mu_{V+} + \mu_{V-})V_i + \mu_{V+}V_{i-1} + \mu_{V-}V_{i+1}, \end{aligned} \quad (2)$$

where  $i = 1, \dots, 588$ , with periodic boundary conditions (see scheme in Fig. 1). The resulting systems is a discretised set of reaction–diffusion equations.

The system of Eq. (2) has two different fixed points. One of the form  $(L_i, T_i, V_i) = (0, 0, 0)$ ,  $\forall i$ , this is the infection-free equilibrium fixed point, and it is a repeller. The other fixed point is of the form  $(L_i, T_i, V_i) = (L_j, T_j, V_j) \neq (0, 0, 0)$ ,  $\forall i, j$  and it is a global attractor. The value of  $V_i$  corresponding to the latter will be referred to as the *average viral load* in the remaining of this paper. The mean-field behaviour is not able to capture the viral blips (see Fig. 5) and noise has to be considered (see Fig. 5).

## 2.3. In silico blood sample analysis model

Further to the compartmental model of Section 2.1 which allows us to account for density fluctuations in stochastic viral dynamics, we have formulated an *In silico* blood sample analysis model. This additional model has the aim of trying to reproduce the experimental procedure described in Nettles et al. (2005) as closely as possible. Nettles et al. (2005) designed an experimental protocol in which ten HIV-1 infected patients under HAART were intensively sampled (every 2 or 3 days) for a period of 3 to 4 months. Each time blood was extracted, two samples per patient were taken and sent to two different laboratories for analysis. They

**Table 3**

Parameter values used in our numerical simulations. The value of  $L_{\max}$  is let to vary depending on the average viral load we impose on our simulations. For the values of the average viral load considered in Section 3, i.e. 10, 12.5, 20, 30, and 40 copies/ml, the corresponding values of  $L_{\max} = 1.89, 2.36, 3.78, 5.66$ , and  $7.55$  cells/ml, respectively.

Parameter	Rate	Description	Reference
$\lambda$	$10,000 \text{ ml}^{-1} \text{ day}^{-1}$	Recruitment rate of T cells	Callaway and Perelson (2002)
$d_T$	$0.0166 \text{ day}^{-1}$	Death rate of T cells	Mohri et al. (1998)
$k$	$2.4 \times 10^{-8} \text{ ml day}^{-1}$	Infection rate	Perelson et al. (1993)
$\epsilon$	0.85	Drug efficacy	Rong and Perelson (2009a)
$\eta$	0.001	Fraction resulting in latency	Jones and Perelson (2007)
$d_0$	$0.001 \text{ day}^{-1}$	Death rate of latently infected cells	Callaway and Perelson (2002)
$a_L$	$0.1 \text{ day}^{-1}$	Rate of transition from latently to productively	Rong and Perelson (2009a)
$\sigma$	$1 \text{ day}^{-1}$	Death rate of productively infected cells	Markowitz et al. (2003)
$c$	$23 \text{ day}^{-1}$	Clearance rate of free virus in blood stream	Ramratnam et al. (1999)
$p_v$	$2000 \text{ day}^{-1}$	Viral production rate	Hockett et al. (1999)
$r$	$0.2 \text{ day}^{-1}$	Proliferation rate of activated cells	Rong and Perelson (2009a)
$L_{\max}$	See caption	Carrying capacity density of latent cells	Rong and Perelson (2009a)
$V_c$	8.5 ml	Compartment volume	Nettles et al. (2005)

concluded that blips had short duration (less than 3 days on average) and low amplitude (79 copies/ml on average) with an average of 1.8 blips per patient.

Our procedure is as follows. After running the compartmental dynamics until time  $t_c$ , which is chosen to be long enough so that the average properties of the system reach a steady state, we choose two compartments at random  $i$  and  $j$  among the  $N_c$  compartments that compose our system. We then record the corresponding state  $x_i(t_c) = (T_i^*(t_c), L_i(t_c), V_i(t_c))$  and  $x_j(t_c) = (T_j^*(t_c), L_j(t_c), V_j(t_c))$ . Recall that we are assuming that the number of uninfected T cells is assumed to be constant and uniform (Conway and Coombs, 2011). In order to account for possible delays between the time of extraction and the actual analysis, we assume that the extracted samples continue to evolve subject to the local (within-compartment) dynamics determined by the rates in Table 1 with the transition rates corresponding to between-compartment transitions  $\omega_l(X) = 0$ . This post-extraction dynamics is ran for a duration  $t_w$ . To reproduce the experimental protocol of Nettles et al. (2005), we choose  $t_c = 2, 4, 6, 9, 11, 13, 16, \dots, 81, 83$  days, since they subtracted the blood each Monday, Wednesday and Friday, during a total of 36 extractions.

#### 2.4. Effects of continuous versus burst production of virions

The issue of whether virions are secreted by active infected cells in a continuous way during their lifespan or, on the contrary, they are released in a single burst which, actually, kills the cell remains controversial. Standard models based on mean-field, deterministic systems of ordinary differential cannot distinguish between both production modes, since they predict exactly the same dynamics as long as the total number of virions produced over their lifespan is the same (Pearson et al., 2011). A recent analysis by Pearson and co-workers has concluded that stochastic models of early infection lead to significantly different results depending on whether virion production is considered as continuous or bursty (Pearson et al., 2011).

Here, we consider this issue regarding its possible influence on the statistics of viral blips. To this end, we consider two models, namely, one in which only continuous virion production is taken into account (given in Table 1) and another one in which both modes of virion production, continuous and bursty, are considered. The latter requires an alteration of the process described by Table 1. The reaction corresponding to active cell death now reads

$$W_{7+(i-1)R_L} = \delta T_i^* \text{ and } r_{7+(i-1)R_L} = (0, -1, N) \quad (3)$$

which implies that upon active cell death, one active cell death is lost and  $N$  virions are released.  $N$  is the so-called burst size. A further modification needs to be done, this time affecting the rate of continuous virion production:

$$W_{9+(i-1)R_L} = p'_v T_i^* \text{ and } r_{9+(i-1)R_L} = (0, 0, 1) \quad (4)$$

where  $p'_v$ , i.e. the rate of continuous virion production, is now a function of the burst size,  $N$ . Given a value of  $N$ , we fix  $p'_v$  so that the average number of virion produced during the lifespan of an active infected cell is the same as for the purely continuous virion production model (i.e.  $N=0$  as per Table 1).

The remaining reactions are left unmodified with respect to those shown in Table 1.

### 3. Results

In this section we will use the models presented in Section 2 to explore the phenomenology associated to our model and obtain statistics of viral blips which can then be compared to the experimental data reported by Nettles et al. (2005). In Fig. 5, we

show the comparison between the mean-field behaviour and one stochastic sample path. This particular sample shows the values of the viral load in the two randomly chosen compartments. This example illustrates how (i) the stochastic model produces blips and (ii) the two different samples show a completely different behaviour, in terms of frequency and duration of viral blips. This behaviour is beyond the reach of both the mean-field model and also of well-mixed stochastic models.

#### 3.1. Effect of density fluctuations on blips statistics

We have carried out extensive numerical simulations of our model using the methodology explained in Section 2. We start by focusing in our inhomogeneous infection model with continuous virion production as defined by the transition rates given in Table 1, accounting for the local infection dynamics, and 2, accounting for diffusion of cells/virions between compartments. Results are included in Figs. 2, 3 and 4.

Nettles et al. (2005) reported that 9 out of 10 patients who underwent their intensive sampling protocol were observed to exhibit at least one blip. In other words, the probability of detecting at least one blip during the course of their experiments can be estimated to be 90%. By means of numerical simulations of our *in silico* blood sample model, we have computed the probability of detecting at least one blip as a function of the average viral load (see Fig. 2, burst size  $N=0$ ). Our results show that, as the average viral load grows, so does the probability of detecting at least one blip. According to our results for viral loads bigger than 20 copies/ml, this probability approaches 1, in good agreement with figure reported in Nettles et al. (2005).

Nettles et al. (2005) reported further statistical information, in particular, regarding blip duration (reproduced in Fig. 3) by recording the frequency with which blips of a certain duration are observed. They observed the blips with duration of 3 days or shorter accounted for over 80% of the observations. Blips of duration between 3 and 5 days, 5 and 7 days and of 7 days or longer were observed in less than 10% of the cases each. Our simulation results are in good agreement with these observations (see Fig. 3). Our model, however, appears to overestimate the

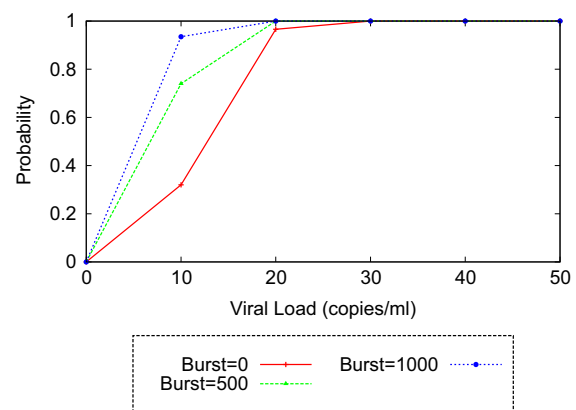


**Fig. 2.** Average of 1000 Gillespie simulations. Probability of observing at least one blip in our *in silico* blood sample analysis model as a function of the average virus load for different values of the burst size. Nettles et al. (2005) in their intensive sampling study showed that 9 out of 10 patients underwent at least one viral blip. We observe that, as the average viral load increases the probability of observing at least one blip tends to one. We also observe that as the burst size increases the observation of at least one blip becomes more likely. Note that the rate of continuous virion production has been chosen for each value of the burst size so that the average number of virions produced per active infected cell during its lifetime is kept constant. Parameter values as per Table 3.  $p'_v$  is taken such that  $p'_v + \delta N = p_v$ , where  $N$  is the burst size and  $p_v$  is given in Table 3.

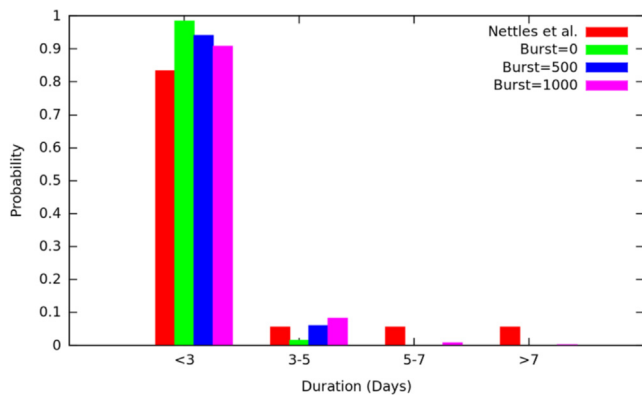


**Fig. 3.** Average of 1000 Gillespie simulations. Comparison between blips statistics obtained in the study by Nettles et al. (2005) and those obtained from our simulations for different burst sizes. This plot shows the probability of observing a blip of a given duration (measured in days). The rate of continuous virion production has been chosen for each value of the burst size so that the average number of virions produced per active infected cell during its life-time is kept constant. We have fixed an average viral load of 12.5 copies/ml (Nettles et al., 2005). Parameter values as per Table 3.  $p'_v$  is taken such that  $p'_v + \delta N = p_v$ , where  $N$  is the burst size and  $p_v$  is given in Table 3.

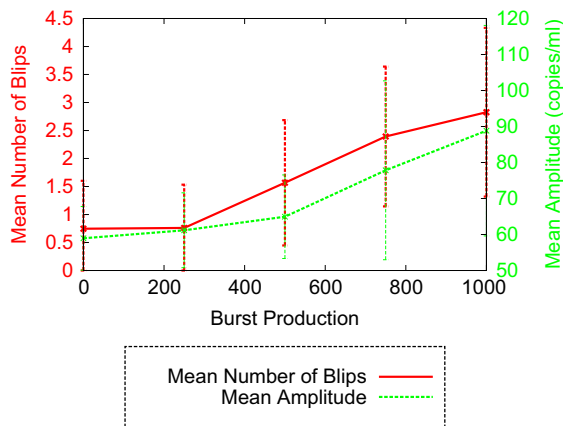


**Fig. 4.** Average of 1000 Gillespie simulations. This plot shows the average number of blips and median amplitude as a function of the burst size obtained with our model. According to Nettles et al. (2005), the average number of blips per patient is 1.7 and the median of the amplitude is 79 copies/ml. The rate of continuous virion production has been chosen for each value of the burst size so that the average number of virions produced per active infected cell during its life-time is kept constant. We have fixed an average viral load of 12.5 copies/ml (Nettles et al., 2005). Parameter values as per Table 3.  $p'_v$  is taken such that  $p'_v + \delta N = p_v$ , where  $N$  is the burst size and  $p_v$  is given in Table 3.

frequencies of the shorter blips (duration of 3 days or shorter and between 3 and 5 days) at the expense of the longer ones.

Further information that can be extracted from the data reported in Nettles et al. (2005) concerns the average number of blips and their average amplitude. According to their experiments, the average number of blips is 1.8 and their average amplitude 79 copies/ml. Regarding these two metrics, our simulation results reported in Fig. 4 for burst size equal to zero show that our inhomogeneous infection model with continuous virion production underestimates these quantities by a significant amount.

### 3.2. Effect of burst production of virions

In order to improve the quantitative agreement between the data reported in Nettles et al. (2005) and our model predictions,

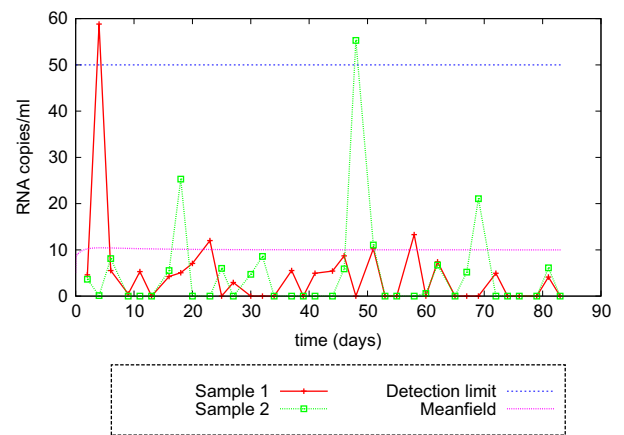


**Fig. 5.** A comparison between the mean-field dynamics and a realisation of the stochastic process with. We observe that the mean-field goes to the metastable state, whilst the stochastic simulations capture the viral blips. However, the dynamics of the two samples of the stochastic process are completely different. Parameter values as per Table 3.  $p'_v$  is taken such that  $p'_v + \delta N = p_v$ , where  $N=1000$  is the burst size and  $p_v$  is given in Table 3,  $t_w=0$ ,  $L_{max}=1.89$ .

we have explored the effect of including both continuous and burst virion production (see Section 2.4). In particular, we have analysed the behaviour of our system as a function of the burst size, keeping constant the average number of virions produced by active infected cells during their lifespan.

We have studied the effect of burst production on the statistics concerning viral blips shown in Figs. 2–4. Regarding the probability of detecting at least one blip, although its behaviour for positive burst size is qualitatively similar to the burst size  $N=0$  case, our model predicts an increase in the probability of observing at least one blip for lower values of the average viral load (see Fig. 2). This increase is proportional to the burst size: The bigger the burst size, the larger the increase in the probability of observing at least one blip.

We observe that the frequency of viral blips increases as the burst size increases, under conditions of constant mean total number of produced virions. This effect can be explained in stochastic terms as follows: whilst the mean total number of produced virions the average rate of virion production increases with the portion allocated to burst at cell death,  $B$ . A little analysis shows that the number of virus produced by continuous viral production is geometric, with median production of virions being an increasing function of the burst size,  $B$ . Therefore, while the mean number of produced virions is the same, because of the large amounts of virions produced at burst events production, the average production rate increases.

The discrepancies between experimental data and simulation results concerning the frequency of blip duration tend to be corrected when a positive burst size is considered (see Fig. 3). As we have discussed previously, the inhomogeneous infection model with continuous virion production overestimates the frequency of shorter blips at the expense of longer ones. This trend is compensated when we consider burst production of virions: As the burst size is let to increase, shorter blips become less frequent at the expense of longer ones, whose frequency is observed to increase as shown in Fig. 3.

Further discrepancies between the data reported in Nettles et al. (2005) and simulation results of our inhomogeneous infection model with continuous virion production regarding the average number of blips and their average amplitude. Our model with no burst virion production underestimates these quantities. Fig. 4 shows that, as burst size increases, the value predicted by our model for these two quantities approaches those reported in Nettles et al. (2005).



To summarise, although our inhomogeneous infection model with continuous virion production appears to qualitatively capture the blip statistics obtained by Nettles et al. (2005), better quantitative agreement is obtained when burst production of virions is considered.

### 3.3. Effect of post-extraction handling time

A controversial aspect regarding the origin and clinical significance of viral blips is the claim that their statistics are affected by artifacts related to the sample manipulation process (Lee et al., 2006; Nettles and Kieffer, 2006). In order to partially address this issue within the context of our model, we have devised a set of simulations in which we consider the effect of the post-extraction handling

time in our *in silico* blood test model,  $t_w$  (see Section 2.3). This time is assumed to correspond to the time elapsed between extraction of the blood sample and actual analysis at the laboratory. We have considered that  $t_w$  is of the order several hours. During this time lapse, the infection dynamics stays running but since the sample is now extracted and therefore isolated there is no between-compartments cell/virion motility (i.e. the dynamics is described by a purely local infection model determined by the rates given in Table 1). Extraction of a compartment (sample) and its consequent isolation from the blood stream has the likely effect of reducing the rate at which virus particles are cleared, since it has been isolated from usual removal mechanisms. We have therefore considered the effect of reducing the virus clearance rate with respect to current

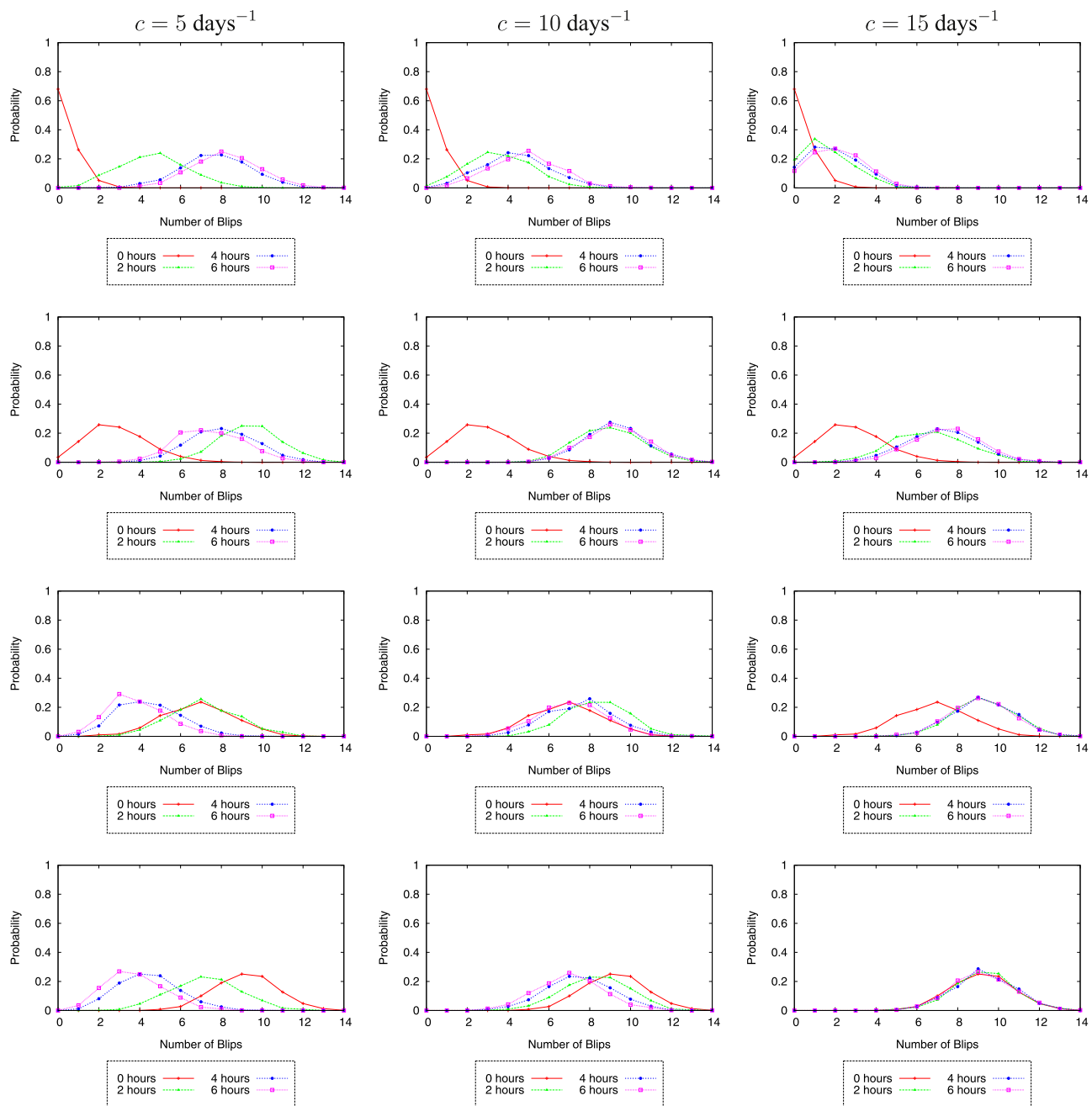


**Fig. 6.** Average of 1000 Gillespie simulations. Probability of observing  $n$  blips within a sample,  $P(n)$ , as a function of the post-extraction handling time,  $t_w$ , and the virus clearance rate,  $c$ . We have also considered different value of the average viral load: the first, second, third, and fourth correspond to 10, 20, 30, and 40 copies/ml, respectively. We have considered the continuous virion production only.

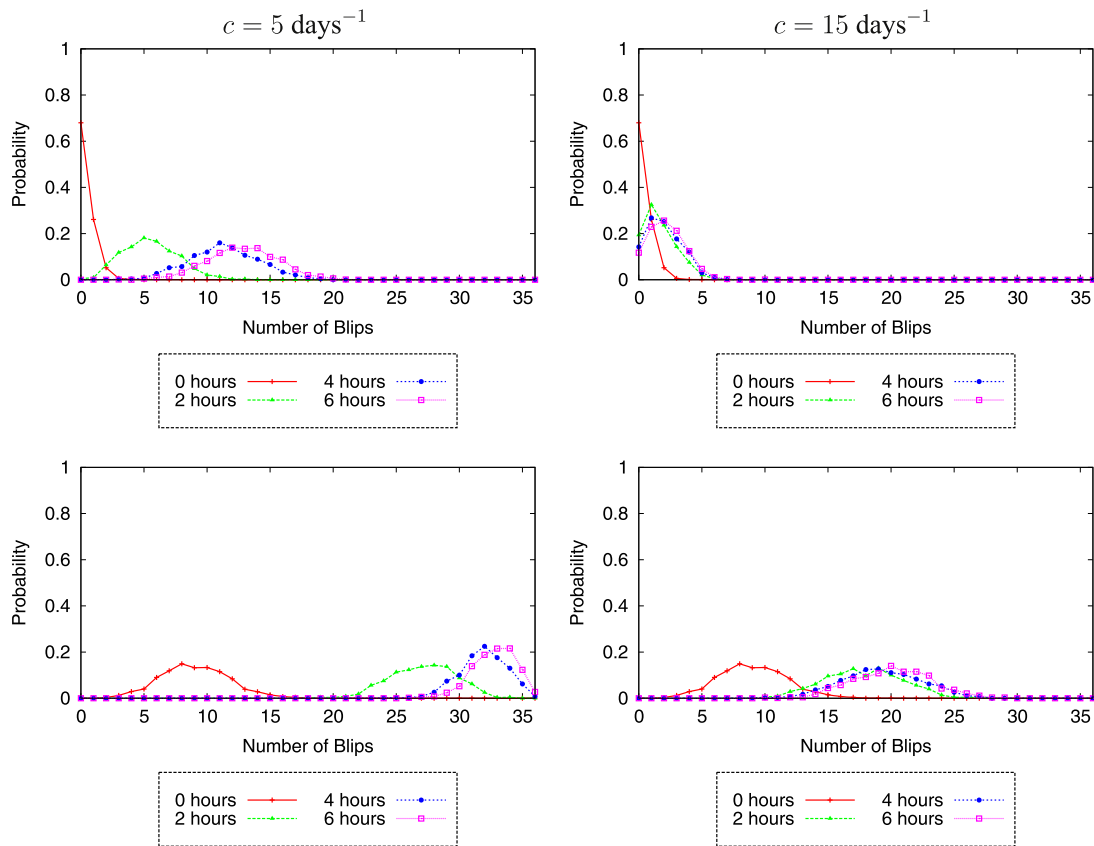


**Fig. 7.** Average of 1000 Gillespie simulations. Probability of having  $n$  observations above the detection limit within a sample,  $P(n)$ , as a function of the post-extraction handling time,  $t_w$ , and the virus clearance rate,  $c$ . We have also considered different value of the average viral load: The first, and second correspond to 10 and 40 copies/ml, respectively. We have considered the continuous virion production only.

estimates in the literature (see Table 3). Note that all the simulation results presented in Sections 3.1 and 3.2 correspond to  $t_w=0$ .

In order to assess the effects of both the handling time,  $t_w$ , and the virus clearance rate,  $c$ , we have done numerical simulations to compute the Probability of observing  $n$  blips within a sample,  $P(n)$ , for different values of the average viral load. Our results are reported in Fig. 6. For lower values of the average viral load (see Fig. 6, 10 and 20 copies/ml), we observe that there is a strong dependence on the average number of blips with  $t_w$ : Due to accumulation of virus capsids as time progresses (recall that we are assuming that active infected cells continue to release virions after extraction until such time as the actual count is carried out), the average number of blips increases, as indicated by the fact that the peak of  $P(n)$  shifts to larger values of  $n$  as  $t_w$  increases. Likewise, the position of this peak shifts to larger values of  $n$  as the virus clearance rate,  $c$ , decreases. For larger values of the average viral load (see Fig. 6, 30 and 40 copies/ml), our simulation results show that the peak of  $P(n)$  shifts to smaller values of  $n$  as  $t_w$  increases. This result is actually an artifact of how blips are defined and counted: A blip is the event whereby the viral load, initially below 50 copies/ml, transiently grows above the detection threshold. When the average viral load is 30 or 40 copies/ml, the duration of these events becomes very long, which has the by-product of reducing the blips count. To illustrate this phenomenon, we show in Fig. 7 the number of observations which are above 50 RNA copies/ml. When the viral load is 10 copies/ml, the difference between the number of observations above the detection limit and the number of viral blips is small. However, in the case of 40 copies/ml we see strong discrepancies between both pictures. Although the viral load is most of time above 50 copies/ml, we are considering most of that observations as the same viral blip

and, in this case, the number of viral blips is given by the number of observations below the detection limit.

#### 4. Discussion

The aim of this paper is to contribute to the discussion of whether viral blips in HIV-1 infected patients treated with HAART are symptomatic of ensuing drug failure or if, on the contrary, they are random occurrences uncorrelated to drug-efficiency status and therefore lacking clinical significance. To this end, we have presented an inhomogeneous stochastic HIV-1 infection dynamics model, based on previous mean-field and stochastic models (Rong and Perelson, 2009a; Conway and Coombs, 2011), which accounts for local density fluctuations and burst virion production. Previous models (Rong and Perelson, 2009a; Conway and Coombs, 2011) assume that the system is well-stirred and, therefore, homogeneous. Given the small number of individuals involved in our model, in particular, regarding the number of virus copies during the latent infection phase, we have hypothesised that spatial inhomogeneities may play a role.

We have proposed a stochastic infection model which extends the model proposed in Conway and Coombs (2011) by accounting for density inhomogeneities and bursty virion production. We have avoided the consideration of factors such as random activation of latently infected cells or upregulated virion production rate which have been introduced in previous models (Rong and Perelson, 2009a; Conway and Coombs, 2011). We have further designed an *in silico* blood sample model, in order to reproduce as faithfully as possible the experimental protocol of Nettles et al. (2005). By doing so, we have been able to show that our model closely reproduces the blip statistics obtained in Nettles et al. (2005),

in particular when burst virion production is considered (see Figs. 2, 3 and 4), thus supporting the hypothesis that viral blips in HAART-treated patients are random events unrelated to drug failure (Lee et al., 2006; Nettles and Kieffer, 2006).

Previous modelling approaches have made different claims regarding the origin of blips. Rong and Perelson (2009a) have postulated that random activation of latently infected cells by exposure to the corresponding antigens account for the presence of blips in HAART-treated patients. Conway and Coombs (2011) have formulated a model in which a heightened rate of virion production is necessary for their model to reproduce realistic values of blip frequency, which could be interpreted as blips being the consequence of an evolutionary process where new variants of the virus have emerged with an increased virion production rate. Whilst our model does not disprove any of these mechanisms as well as others proposed in the literature (Ferguson et al., 1999; Gunthard et al., 2000; Frazer et al., 2001; Fraser et al., 2001; Frenkel et al., 2003; Jones and Perelson, 2002, 2005; Macias et al., 2005), our model points out that viral blips may be purely random occurrences uncorrelated with factors of clinical significance.

Furthermore, our approach allows us to (partially) address the issue of whether laboratory and sample manipulation artifacts affect the observation of blips (Lee et al., 2006; Nettles and Kieffer, 2006). We have investigated the effect that the post-extraction handling time, i.e. the time elapsed between sample extraction and the actual analysis, has on the statistics of the number of blips. According to our model, this factor contaminates the statistics of the number and duration of blips (see Fig. 6), which supports the aforementioned position regarding the effects laboratory artifacts on viral blip observation. However, our model of the post-extraction dynamics is still largely speculative. A more thorough of the multiple factors that may affect it, such as, for example, how sample refrigeration affects the infection dynamics, requires a careful and more detailed study that is beyond the scope of this paper. We leave the analysis of such issues for future work.

## Acknowledgements

The authors gratefully acknowledge the Spanish Ministry for Science and Innovation (MICINN) for funding under Grant MTM2011-29342 and Generalitat de Catalunya for funding under Grant 2009SGR345. We also would like to thank one anonymous referee for suggesting a stochastic argument to explain the behaviour of the blip frequency with varying burst size.

## References

Alarcon, T., Jensen, H.J., 2010. Quiescence: a mechanism for escaping the effects of drug on cell populations. *J. R. Soc. Interface* 8, 99–106.

Berg, H.C., 1993. *Random Walks in Biology*. Princeton University Press, Princeton, NJ, USA.

Bernstein, D., 2005. Simulating mesoscopic reaction–diffusion systems using the Gillespie algorithm. *Phys. Rev. E* 71, 041103.

Bray, D., 2001. *Cell Movements: From Molecules to Motility*. Garland Publishing, New York, NY, USA.

Callaway, D.S., Perelson, A.S., 2002. HIV-1 infection and low steady state viral loads. *Bull. Math. Biol.* 64 (1), 29–64.

Chomont, N., El-Far, M., Ancuta, P., Trautmann, L., Procopio, F.A., Yassine-Diab, B., Boucher, G., Boulassel, M.-R., Brechley, J.M., Schacker, T.W., Hill, B.J., Ghattas, D.C.D.G., Routy, J.-P., Haddad, E.K., Sekaly, R.-P., 2009. HIV reservoir size and persistence are driven by T cell survival and homeostatic proliferation. *Nat. Med.* 15, 893–901.

Chun, T.W., Finzi, D., Margolick, J., Chadwick, K., Schwartz, D., Siliciano, R.F., 1995. In vivo fate of HIV-1-infected T cells: quantitative analysis of the transition to stable latency. *Nat. Med.* 1, 1284–1290.

Chun, T.-W., Carruth, L., Finzi, D., Shen, X., DiGiuseppe, J.A., Taylor, H., Hermankova, M., Chadwick, K., Margolick, J., Quinn, T.C., Kuo, Y.-H., Brookmeyer, R., Zeiger, M.A., Barditch-Crovo, P., Siliciano, R.F., 1997. Quantification of latent tissue reservoirs and total body viral load in HIV-1 infection. *Nature* 387, 183–188.

Conway, J.M., Coombs, D., 2011. A stochastic model of latently infected cell reactivation and viral blip generation in treated HIV patients. *PLoS Comput. Biol.* 7, e1002033.

DiMascio, M., Markowitz, M., Louie, M., Hogan, C., Hurley, A., Chung, C., Ho, D.D., Perelson, A.S., 2003. Viral blip dynamics during highly active antiretroviral therapy. *J. Virol.* 77 (22), 12165–12172.

Dornadula, G., Zhang, H., VanUitert, B., et al., 1999. Residual HIV-1 RNA in blood plasma of patients taking suppressive highly active antiretroviral therapy. *JAMA* 282 (17), 1627–1632.

Elf, J., Ehrenberg, M., 2004. Spontaneous separation of bi-stable biochemical systems into spatial domains of opposite phases. *Syst. Biol.* 1, 230–235.

Elgart, V., Kamenev, A., 2004. Rare event statistics in reaction–diffusion systems. *Phys. Rev. E* 70, 041106.

Erbani, R., Chapman, J., Maini, P. A practical guide to stochastic simulations of reaction–diffusion processes, arXiv preprint arXiv: arXiv:0704.1908.

Ferguson, N.M., deWolf, F., Ghani, A.C., Fraser, C., Donnelly, C.A., Reissi, P., Langei, J.M.A., Danner, S.A., Garnett, G.P., Goudsmit, J., Anderson, R.M., 1999. Antigen-driven CD41 T cell and HIV-1 dynamics: residual viral replication under highly active antiretroviral therapy. *Proc. Natl. Acad. Sci. USA* 96, 15167–15172.

Fraser, C., Ferguson, N.M., Anderson, R.M., 2001. Quantification of intrinsic residual viral replication in treated HIV infected patients. *Proc. Natl. Acad. Sci. USA* 98, 15167–15172.

Frazer, C., Ferguson, N.M., de Wolf, F., Anderson, R.M., 2001. The role of antigenic stimulation and cytotoxic T cell activity in regulating the long-term immunopathogenesis of HIV: mechanisms and clinical implications. *Proc. R. Soc. Lond. B* 268, 2085–2095.

Frenkel, L.M., Wang, Y., Learn, G.H., McKernan, J.L., Ellis, G.M., Mohan, K.M., Holte, S.E., Vange, S.M.D., Pawluk, D.M., Melvin, A.J., Lewis, P.F., Heath, L.M., Beck, I.A., Mahalanabis, M., Naugler, W.E., Tobin, N.H., Mullins, J.L., 2003. Multiple viral genetic analyses detect low-level human immunodeficiency virus type 1 replication during effective highly active antiretroviral therapy. *J. Virol.* 77, 5721–5730.

Gardiner, C.W., 2009. *Stochastic Methods*. Springer-Verlag, Berlin, Germany.

Gibson, M.A., Bruck, J., 2000. Efficient exact stochastic simulation of chemical systems with many species and many channels. *J. Phys. Chem. A* 104, 1876–1889.

Gillespie, D.T., 1976. A general method for numerically simulating the stochastic time evolution of coupled chemical reactions. *J. Comput. Phys.* 22, 403–434.

Gunthard, H.F., Wong, J., Spina, C.A., Ignacio, C., Kwok, S., Christopherson, C., Hwang, J., Haubrich, R., Havlir, D., Richman, D.D., 2000. Effect of influenza vaccination on viral replication and immune response in persons infected with human immunodeficiency virus receiving potent antiretroviral therapy. *J. Infect. Dis.* 181, 522–531.

Havlir, D.V., Bassett, R., Levitan, D., Gilbert, P., Tebas, P., Collier, A.C., Hirsch, M.S., Ignacio, C., Condra, J., Günthard, H.F., Richman, D.D., Wong, J.K., 2001. Prevalence and predictive value of intermittent viremia with combination HIV therapy. *JAMA* 286, 171–179.

Herz, A.V.M., Bonhoeffer, S., Anderson, R.M., May, R.M., Nowak, M.A., 1996. Viral dynamics in vivo: limitations on estimates of intracellular delay and virus decay. *Proc. Natl. Acad. Sci. USA* 93, 7247–7251.

Hille, B., 1992. *Ionic Channels of Excitable Membranes*. Sinauer Associates, Sunderland, MA, USA.

Hockett, R.D., Kilby, J.M., Derdeyn, C.A., Saag, M.S., Sillers, M., Squires, K., Chiz, S., Nowak, M.A., Shaw, G.M., Bucy, R.P., 1999. Constant mean viral copy number per infected cell in tissues regardless of high, low, or undetectable plasma HIV RNA. *J. Exp. Med.* 189 (10), 1545–1554.

Ho, D.D., Rota, T.R., Hirsch, M.S., 1986. Infection of monocyte/macrophages by human T lymphotropic virus type III. *J. Clin. Invest.* 77, 1712–1715.

Ho, D.D., Neumann, A.U., Perelson, A.S., Chen, W., Leonard, J.M., Markowitz, M., 1995. Rapid turnover of plasma virions and CD4 lymphocytes in HIV-1 infection. *Nature* 373, 123–126.

Jones, L.E., Perelson, A.S., 2002. Modelling the effects of vaccination on chronically infected HIV-positive patients. *J. Acquir. Immune Defic. Syndr.* 31, 369–377.

Jones, L.E., Perelson, A.S., 2005. Opportunistic infections as a cause of transient viremia in chronically infected HIV patients under treatment with HAART. *Math. Biosci.* 67, 1227–1251.

Jones, L.E., Perelson, A.S., 2007. Transient viremia, plasma viral load and reservoir replenishment in HIV-infected patients on antiretroviral therapy. *J. Acquir. Immune Defic. Syndr.* 45, 483–493.

Kepler, T.B., Perelson, A.S., 1998. Drug concentration heterogeneity of drug resistance facilitates the evolution of drug resistance. *Proc. Natl. Acad. Sci. USA* 95, 11514–11519.

Kim, H., Perelson, A.S., 2006. Viral and latent reservoir persistence in HIV-1-infected patients on therapy. *PLoS Comput. Biol.* 2, e135.

Lee, P.K., Kieffer, T.L., Siciliano, R.F., Nettles, R.E., 2006. HIV-1 viral load blips are of limited clinical significance. *J. Antimicrob. Chemother.* 57, 803–805.

Lugo, C., McKane, A.J., 2008. Quasicycles in a spatial predator–prey model. *Phys. Rev. E* 78, 051911.

Macias, J., Palomares, J.C., Mira, J.A., Torres, M.J., Garcia-Garcia, J.A., Rodriguez, J.M., Vergera, S., Pineda, J.A., 2005. Transient rebounds of HIV plasma viremia are associated with the emergence of drug resistance mutations in patients of highly active antiretroviral therapy-. *J. Infect.* 5, 195–200.

Markowitz, M., Louie, M., Hurley, A., Sun, E., Mascio, M.D., Perelson, A.S., Ho, D.D., 2003. A novel antiviral intervention results in more accurate assessment of human immunodeficiency virus type 1 replication dynamics and T-cell decay in vivo. *J. Virol.* 77, 5037–5038.

- Mira, J.A., Macias, J., Nogales, C., Fernandez-Rivera, J., Garcia-Garcia, J.A., Ramos, A., Pineda, J.A., 2002. Transient rebounds of low-level viraemia among HIV-infected patients under HAART are not associated with virological or immunological failure. *Antivir. Ther.* 7, 251–256.
- Mohri, H., Bonhoeffer, S., Monard, S., Perelson, A.S., Ho, D.D., 1998. Rapid turnover of T lymphocytes in SIV-infected rhesus macaques. *Science* 279 (5354), 1223–1227.
- Murray, A.G., Jackson, G.A., 1992. Viral dynamics: a model of the effects of size shape, motion and abundance of single-celled planktonic organisms and other particles. *Mar. Ecol. Progr. Ser.* 89, 103–116.
- Nettles, R.E., Kieffer, T.L., 2006. Update on HIV-1 viral load blips. *Curr. Opin. HIV & AIDS* 1, 157–161.
- Nettles, R.E., Kieffer, T.L., Daphne Monie, P.K., Han, Y., Parsons, T., Cofrancesco, J., Gallant, J.E., Quinn, T.C., Jackson, B., Flexner, C., Carson, K., Ray, S., Persaud, D., Siliciano, R.F., 2005. Intermittent HIV-1 viremia (blips) and drug resistance in patients receiving HAART. *JAMA* 293, 817–829.
- Pearson, J.E., Krapivsky, P., Perelson, A.S., 2011. Stochastic theory of early viral infection: continuous versus burst production of virions. *PLoS Comput. Biol.* 7, e1001058.
- Perelson, A.S., Kirschner, D.E., De Boer, R., 1993. Dynamics of HIV infection of CD4+ T cells. *Math. Biosci.* 114 (1), 81–125.
- Perelson, A.S., Neumann, A.U., Markowitz, M., Leonard, J.M., Ho, D.D., 1996. HIV-1 dynamics in vivo: virion clearance rate, infected cell life-span, and viral generation time. *Science* 271, 1582–1586.
- Perelson, A.S., Essunger, P., Cao, Y., Vesanen, M., Hurley, A., Saksela, K., Markowitz, M., Ho, D.D., 1997. Decay characteristics of HIV-1-infected compartments during combination therapy. *Nature* 387, 188–191.
- Pierson, T., McArthur, J., Siliciano, R.F., 2000. Reservoirs for HIV-1: mechanisms for viral persistence in the presence of antiviral immune response and antiretroviral therapy. *Annu. Rev. Immunol.* 18, 665–708.
- Ramratnam, B., Bonhoeffer, S., Binley, J., Hurley, A., Zhang, L., et al., 1999. Rapid production and clearance of HIV-1 and hepatitis C virus assessed by large volume plasma apheresis. *Lancet* 354, 1782–1785.
- Richman, D.D., Margolis, D.M., Delaney, M., Greene, W.C., Hazuda, D., Pomerantz, R.J., 2009. The challenge of finding a cure for HIV infection. *Science* 323, 1304–1307.
- Rong, L., Perelson, A.S., 2009a. Modeling latently infected cell activation: viral and latent reservoir persistence, and viral blips in HIV-infected patients on potent therapy. *PLoS Comput. Biol.* 5, e1000533.
- Rong, L., Perelson, A.S., 2009b. Modelling HIV persistence, the latent reservoir, and viral blips. *J. Theor. Biol.* 260, 308–331.
- Rong, L., Perelson, A.S., 2009c. Asymmetric cell division of activated latently infected cells may explain the decay kinetics of the HIV-1 latent reservoir and intermittent viral blips. *Math. Biosci.* 217, 77–87.
- Siliciano, J.D., Kajdas, J., Finzi, D., Quinn, T.C., Chadwick, K., Margolick, J.B., Kovacs, C., Gange, S.J., Siliciano, R.F., 2003. Long-term follow-up studies confirm the stability of the latent reservoir for HIV-1 in resting CD4+ T cells. *Nat. Med.* 9, 727–728.
- Spill, F., Guerrero, P., Alarcón, T., Maini, P.K., Byrne, H.M., 2015. Mesoscopic and continuum modelling of angiogenesis. *J. Math. Biol.* 70, 485–532. <http://dx.doi.org/10.1007/s00285-014-0771-1>.
- Tsoularis, A., Wallace, J., 2002. Analysis of logistic growth models. *Math. Biosci.* 179 (1), 21–55.
- Van Kampen, N.G., 2007. *Stochastic Processes in Physics and Chemistry*. Elsevier, The Netherlands.
- Wang, S., Rong, L., 2014. Stochastic population switch may explain the latent reservoir stability and intermittent viral blips in HIV patients on suppressive therapy. *J. Theor. Biol.* 360, 137–148.
- Wei, X., Ghosh, S.K., Taylor, M.E., Johnson, V.A., Emini, E.A., Deutsch, P., Lifson, J.D., Bonhoeffer, S., Nowak, M.A., Hahn, B.H., Saag, M.S., Shaw, G.M., 1995. Viral dynamics in human immunodeficiency virus type 1 infection. *Nature* 373, 117–122.
- Zhang, Z.-Q., Schuler, T., Zupancic, M., Wietgreffe, S., Staskus, K.A., Reimann, K.A., Reinhart, T.A., Rogan, M., Cavert, W., Miller, C.J., Veazey, R.S., Notermans, D., Little, S., Danner, S.A., Richman, D.D., Havlir, D., Wong, J., Jordan, H.L., Schacker, T.W., Racz, P., Tenner-Racz, K., Letvin, N.L., Wolinsky, S., Haase, A.T., 1999. Sexual transmission and propagation of SIV and HIV in resting and activated CD4+ T cells. *Science* 286, 1712–1715.